Xenon Attenuates Hippocampal Long-term Potentiation by Diminishing Synaptic and Extrasynaptic *N*-methyl-D-aspartate Receptor Currents

Stephan Kratzer, M.D.,* Corinna Mattusch, M.Sc.,† Eberhard Kochs, M.D.,‡ Matthias Eder, Ph.D.,§ Rainer Haseneder, M.D.,‖ Gerhard Rammes, Ph.D.#

ABSTRACT

Background: The memory-blocking properties of general anesthetics are of high clinical relevance and scientific interest. The inhalational anesthetic xenon antagonizes *N*-methyl-D-aspartate (NMDA) receptors. It is unknown if xenon affects long-term potentiation (LTP), a cellular correlate for memory formation. In hippocampal brain slices, the authors investigated in area CA1 whether xenon affects LTP, NMDA receptor-mediated neurotransmission, and intracellular calcium concentrations.

Methods: In sagittal murine hippocampal brain slices, the authors investigated the effects of xenon on LTP by recording excitatory postsynaptic field potentials. Using fluorometric calcium imaging, the authors tested the influence of xenon on calcium influx during high-frequency stimulation. In addition, using the patch-clamp technique, the xenon effect on synaptic and extrasynaptic NMDA receptors and L-type calcium channels was examined.

Results: In the absence of xenon, high-frequency stimulation reliably induced LTP and potentiated field potential slopes to (mean ± SEM) 127.2 ± 5.8% ($P < 0.001$). In the presence of xenon, high-frequency stimulation induced only a short-term potentiation, and field potentials returned to baseline level after 15–20 min (105.9 ± 2.9%; $P = 0.090$). NMDA receptor-mediated excitatory postsynaptic currents were reduced reversibly by xenon to 65.9 ± 9.4% ($P = 0.007$) of control. When extrasynaptic receptors were activated, xenon decreased NMDA currents to 58.2 ± 5.8% ($P < 0.001$). Xenon reduced the increase in intracellular calcium during high-frequency stimulation without affecting L-type calcium channels.

Conclusions: *N*-methyl-D-aspartate receptor activation is crucial for the induction of CA1 LTP. Thus, the depression of NMDA receptor-mediated neurotransmission presumably contributes to the blockade of LTP under xenon. Because LTP is assumed to be involved in learning and memory, its blockade might be a key mechanism for xenon's amnestic properties.

What We Already Know about This Topic

- Amnesia is essential for successful anesthesia, but whether xenon, which antagonizes *N*-methyl-D-aspartate (NMDA) receptors, affects hippocampal circuit responses associated with memory formation and storage has not been examined

What This Article Tells Us That Is New

- In hippocampal slices from mice, xenon blocked long-term potentiation, a synaptic and circuit function linked to memory formation by a reduction of NMDA receptor-mediated responses

THE inhibition of both implicit and explicit memory formation is a fundamental component of general anesthesia. A failure of this component may contribute to intraoperative awareness, an adverse event during anesthesia that occurs in a stunningly high number of patients.[1] Despite the clinical importance of the memory-ablating properties of general anesthetics, their neuronal basis remains not entirely clarified.

Memory formation occurs at various sites in the brain. Among other regions,[2] the hippocampus has been suggested to be one of the key structures for anesthetics mediating their amnestic properties.[3] Long-term potentiation (LTP), a long-lasting enhancement of synaptic efficacy upon repetitive and/or simultaneous stimulation of different afferents, represents (especially in the hippocampus) an important and widely studied neuronal correlate for memory formation.[4] A major mechanism of LTP induction is an increased calcium

* Resident in Anesthesia, † Ph.D. Student, ‡ Professor of Anesthesiology, Director and Chair, ‖ Associate Professor, # Professor of Pharmacology and Toxicology, Department of Anesthesiology, Klinikum rechts der Isar, Technische Universität München, Munich, Germany. § Head of the Research Group Neuronal Network Dynamics, Max Planck Institute of Psychiatry, Munich, Germany.

Received from the Department of Anesthesiology, Klinikum rechts der Isar, Technische Universität München, Munich, Germany. Submitted for publication August 11, 2011. Accepted for publication December 7, 2011. Supported in part by grant HA5331/2-2 from the German Research Society (Deutsche Forschungsgemeinschaft), Bonn, Germany. Dr. Kratzer and Ms. Mattusch contributed equally to this article.

Address correspondence to Dr. Kratzer: Department of Anesthesiology, Klinikum rechts der Isar, Technische Universität München, Ismaninger Straße 22, 81675 Munich, Germany. skratzer@mpipsykl.mpg.de. Anesthesiology 2012; 116:673–82

influx through both *N*-methyl-D-aspartate (NMDA) receptors and voltage-gated calcium channels (VGCCs).[5]

An impairment of synaptic plasticity has been reported for several anesthetics. The volatile anesthetics isoflurane[6] and sevoflurane[7] and the intravenous anesthetics propofol[8] and etomidate[9] attenuate hippocampal synaptic plasticity through γ-aminobutyric acid (GABA)-ergic mechanisms. It has been suggested that this effect during the application of the anesthetics may account for the desirable intraoperative amnesia.[6,7,9]

During the last decade, the inhalational anesthetic xenon increasingly came into the focus of clinical and basic research because of its profound anesthetic and analgesic properties and low side effect profile. The safety and efficiency of xenon anesthesia has been evaluated in large clinical trials.[10,11] Pharmacologically, xenon antagonizes NMDA receptors[12] and thus also may affect the induction of LTP.

In the current study, we investigated in the CA1 region of the hippocampus the impact of xenon on LTP, NMDA receptor-mediated neurotransmission, and calcium channel currents in a murine brain slice preparation.

Materials and Methods

Experimental protocols were approved by the Ethical Committee on Animal Care and Use of the Government of Bavaria (Munich, Germany). After male C57BL/6 mice (p20–30) were anesthetized with isoflurane, brains were quickly removed and sagittal slices (350 μm thick), including the hippocampus, were prepared in ice-cold, carbogen-saturated (95% O_2/5% CO_2) artificial cerebrospinal fluid (aCSF; pH 7.4) using a vibratome (HM 650 V; Microm International, Walldorf, Germany). Slices were allowed to recover for at least 1 h at 34°C before being transferred to the recording chamber and continuously perfused with aCSF at a rate of 5 ml/min. The aCSF contained (in mM): NaCl 125, KCl 2.5, $NaHCO_3$ 25, $CaCl_2$ 2, $MgCl_2$ 1, D-glucose 25, NaH_2PO_4 1.25. All experiments were performed at room temperature (23–25°C).

Recordings of field excitatory postsynaptic potentials (fEPSPs) were performed in the CA1 stratum radiatum of the hippocampus using borosilicate glass micropipettes (Clark Electromedical Instruments, Pangbourne Reading, United Kingdom) filled with aCSF, resulting in an open tip resistance of 1–2 MΩ. Data were recorded with an Axopatch 200B patch-clamp amplifier, a Digidata 1200 interface (both from Axon Instruments, Foster City, CA), and the WinLTP Program version 1.11b (WinLTP Ltd., Centre for Synaptic Plasticity, School of Physiology & Pharmacology, University of Bristol, Bristol, United Kingdom).[13] fEPSPs were evoked by alternately delivering a 50-μs voltage pulse *via* one of two bipolar tungsten electrodes (insulated to the tip; 50 μm diameter), placed at either side of the recording pipette, thus stimulating nonoverlapping populations of fibers of the Schaffer collateral-associational commissural pathway (fig. 1). Stimuli of each electrode were delivered alternatively at

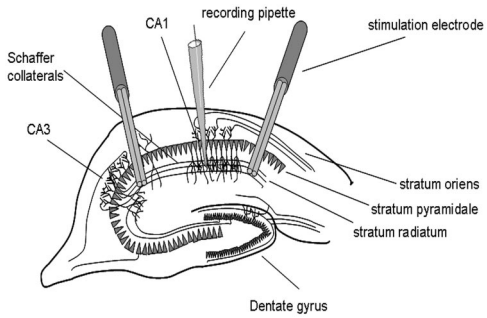

Fig. 1. Schematic drawing of the acute sagittal hippocampal slices. Schaffer collaterals projecting from CA3 to CA1 were stimulated in an antegrade or retrograde manner by two bipolar stimulation electrodes that were positioned in the stratum radiatum. For field potential recordings, the pipette was positioned in the stratum radiatum of the CA1 region of the hippocampus. For patch clamp recordings, CA1 pyramidal neurons were identified and accessed using infrared videomicroscopy. Xenon (1.9 mM) was applied by saturation of the artificial cerebrospinal fluid (aCSF) with xenon (65%) that continuously perfused the whole brain slice.

15-s intervals, and two consecutive fEPSPs were averaged for noise minimization. The slope of the rising phase of the fEPSP (taken between 20 and 80% of the peak amplitude) was used as measure of the strength of synaptic transmission. For baseline recordings, stimulation intensity was adjusted to a value that evoked a response of approximately 25–30% of the maximal obtainable response. For the induction of LTP, a high-frequency stimulation (HFS) train (100 pulses delivered at 100 Hz) was applied to the Schaffer collateral-associational commissural pathway, and subsequent recordings were made for an additional 60 min without changing the stimulation rate and intensity used for baseline recordings. fEPSP slopes were normalized with respect to the responses recorded during the last 5 min before HFS.

Infrared videomicroscopy[14] (Zeiss, Oberkochen, Germany) was used to visualize CA1 pyramidal neurons, from which excitatory postsynaptic currents (EPSCs) were recorded using standard whole cell patch-clamp technique. Pipettes had an open tip resistance of 4–6 MΩ when filled with a solution containing (in mM): K-D-gluconate 130, KCl 5, EGTA 0.5, $MgCl_2$ 2, HEPES 10, D-glucose 5, and Na_2-phosphocreatine 20. Currents were recorded with a switched voltage-clamp amplifier (SEC 10 l; NPI Electronic, Tamm, Germany) with switching frequencies of 60–80 kHz (25% duty cycle). Series resistance was continuously monitored. EPSCs were elicited by square pulse stimuli (6–30 V, 50–500 μs; interstimulus interval 15 s) delivered *via* a bipolar tungsten electrode placed in the Schaffer collateral-associational commissural pathway. Before each tissue stimulation pulse, neuronal input resistance was determined by a hyperpolarizing voltage step (−10 mV for 200 ms). NMDA receptor-mediated EPSCs (NMDA-EPSCs) were recorded in the presence of 1,2,3,4-tetrahydro-6-nitro-2,3-dioxo-benzo[f]quinoxaline-7-sulfonamide (NBQX; 5 μM), 3-

amino-propyl(diethoxymethyl)phosphinic acid (CGP35348; 200 μM), and bicuculline methiodide (20 μM) at a holding potential of −40 mV. At the end of the experiments, we also applied d(-)-2-amino-5-phosphonopentanoic acid (AP5; 50 μM), resulting in a complete blockade of current responses (data not shown). For measurement of α-amino-3-hydroxy-5-methyl-4-isoxazolepropionic acid receptor-mediated currents, NBQX was omitted from the aCSF, and AP5 (50 μM) was added instead.

For measuring the effect of xenon on L-type calcium channels in CA1 pyramidal cells, we substituted calcium in the extracellular solution with barium and thus recorded barium currents through calcium channels. The extracellular solution contained (in mM): NaCl 125, KCl 2.5, $NaHCO_3$ 25, $CaCl_2$ 2, $BaCl_2$ 1, D-glucose 25, NaH_2PO_4 1.25. Pipettes were filled with an intracellular solution containing (in mM): K-D-gluconate 130, KCl 5, EGTA 0.5, $MgCl_2$ 2, HEPES 10, D-glucose 5, and Na_2-phosphocreatine 20. L-type calcium channel currents were recorded by adding specific antagonists to the aCSF: ω-Conotoxin GVIA (1 μM) for N-type channels, ω-Agatoxin IVA (100 nM) for P/Q-type channels and $NiCl_2$ (50 μM) for T-type channels. Barium currents were evoked by a 100-ms depolarizing step from −70 mV to 0 mV.

All current responses were amplified, low-pass filtered (3 kHz), digitized (ITC-16 Computer Interface; Instrutech Corp., Port Washington, NY) with a sampling frequency of 9 kHz, and stored on a hard drive (Power Macintosh G3 computer [Apple, Cupertino, CA], data acquisition software Pulse version 8.5 [HEKA Electronic GmbH, Lambrecht, Germany]).

In a subset of experiments, we measured the intracellular calcium influx during HFS by fluorometric calcium imaging. For this purpose, slices were loaded with the membrane-soluble acetoxymethyl ester of Fluo-4.[15] The dye was dissolved in dimethyl sulfoxide + 20% Pluronic F-127 at a concentration of 5 mM. For slice loading, the solution was diluted 1:10 in a pipette solution containing HEPES-aCSF (in mM: NaCl 125, KCl 3, HEPES 25, $MgSO_4$ 2, $CaCl_2$ 2, NaH_2PO_4 1.25). This resulted in a final dye concentration of 500 μM Fluo-4 acetoxymethyl ester. The dye was applied to the dendrites of hippocampal CA1 neurons by ejecting it from a micropipette (open tip resistance 0.5 MΩ) with a pressure pulse. Cells were allowed to take up the dye for 1 h before the beginning of recordings. Imaging was performed with a ×60 water immersion objective (numerical aperture 0.9; Olympus, Hamburg, Germany) and a filter block containing a 470/40 filter (band pass) and 495 dichroic mirror. A monochromator (Polychrome V; T.I.L.L. Photonics, Martinsried, Germany) was used for excitation with a wavelength of 488 nm, and emission was collected at a maximum of 516 nm. For measurements of calcium-dependent changes in fluorescence, images were sampled during HFS to the Schaffer collateral-associational commissural pathway at 10 Hz for 5 s and recorded with a high-speed, charge-coupled device camera (Retiga-2000RV; QImaging, Surrey, Canada). Data acquisition and offline data analysis were performed with TillVision (T.I.L.L. Photonics). Baseline fluorescence before HFS (F0) and relative fluorescence changes (ΔF/F0) in defined regions of interest were measured throughout the image sequence. Changes in intracellular calcium are expressed as ΔF/F0 × 1,000 using the average of 10 images before HFS as a baseline. The time integral (area under the curve) was used to assess changes in total calcium.

Under control conditions, the aCSF was bubbled with carbogen, whereas for xenon application it was also bubbled with a mixture of 65% xenon, 30% O_2, and 5% CO_2. Concentration measurements of dissolved xenon were accomplished using headspace gas chromatography (Harlan Laboratories Ltd., Itingen, Switzerland). The final concentration of xenon in the aCSF was 1.9 ± 0.5 mM (n = 6). Concentrations of dissolved oxygen and carbon dioxide as well as pH were determined using a calibrated blood gas analyzer (Rapidlab 860 blood gas analyzer; Diamond Diagnostics, Holliston, MA) and did not change during application of the xenon gas mixture. All gas mixtures were purchased from Linde AG (Unterschleissheim, Germany) and applied at a flow rate of 0.3–0.5 l/min to the aCSF reservoir. Tubing was made of polytetrafluoroethylene (Teflon; VWR International, Darmstadt, Germany) to minimize loss of xenon.

All salts and chemicals were purchased from Sigma–Aldrich (Munich, Germany), except CGP35348 (Novartis Laboratories, Basel, Switzerland), and Fluo-4 acetoxymethyl ester (Invitrogen GmbH, Darmstadt, Germany).

Statistical Analysis

For all statistical evaluations, SPSS Statistics version 16 (SPSS GmbH Software, Munich, Germany) was used. The recording times of fEPSPs, NMDA-EPSCs, and calcium channel currents were first portioned in equidistant subintervals of 5-min length. The averaged relative charge, slope, and amplitude were calculated for each of them. Two factorial multivariate analyses of variance with repeated measures design were applied on the averaged relative charge, slopes, and amplitudes with interval as a within-subjects factor and set of experiments as a between-subjects factor. Differences between the various intervals were studied by tests with contrasts, whereas differences between the various experiments by Bonferroni *post hoc* tests. Multivariate analysis of variance was also performed for testing differences in the area under the curve of relative changes in fluorescence during HFS between the control and xenon recordings. In contrast to some other multivariate analyses, multivariate analysis of variance is robust against violations of the normality and homogeneity conditions. Multivariate analysis of variance is based on F-tests, which are, unlike some other parametric tests, very robust against the aforementioned conditions. We accepted $\alpha = 0.05$ as the nominal level of significance. It was corrected (according to Bonferroni procedure) for all *a posteriori* tests (tests with contrasts and *post hoc* tests). Numerical

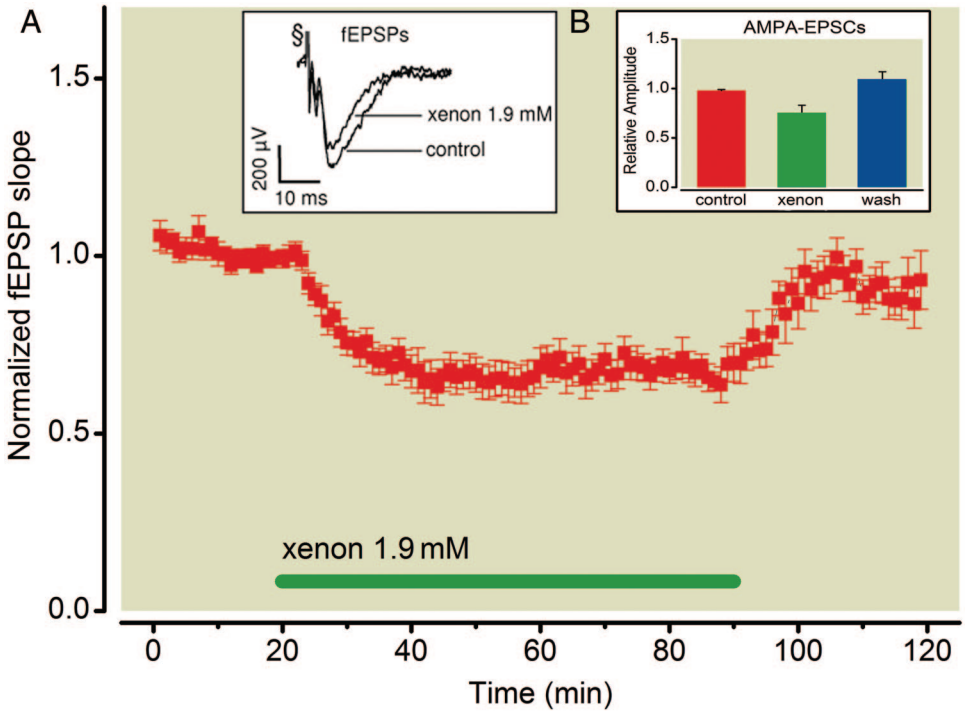

Fig. 2. Xenon diminishes hippocampal CA1 stratum radiatum basal synaptic transmission. Field excitatory postsynaptic potentials (fEPSPs) were evoked by electrical stimulation of the Schaffer collateral-associational commissural pathway and recorded in the CA1 stratum radiatum. Xenon (1.9 mM) caused a stable and reversible reduction of fEPSP slopes to 70.4 ± 3.5% (95% CI 63.6–77.5; n = 7; $P = 0.001$) after 15 min of xenon delivery (*A*). Each *data point* represents the mean ± SEM of four consecutive fEPSP slope measurements normalized to the last 5 min before xenon application. The presence of xenon (*green bar*). Representative recording traces (*left inset*). Because fEPSPs are mediated primarily by α-amino-3-hydroxy-5-methyl-4-isoxazolepropionic acid (AMPA) receptors under physiologic conditions, we investigated the effect of xenon on AMPA receptor-mediated excitatory postsynaptic currents (AMPA-EPSCs). Xenon reversibly reduced AMPA-EPSCs to 75.2 ± 6.6% (95% CI 55.6–94.8; n = 6; $P = 0.013$; *B*). § Stimulation artifact.

data are presented as means ± SEM with the number of experiments indicated, if not stated otherwise. When error bars were smaller than the size of the symbols, they are not shown in the graphs.

Results

In a first set of experiments, we determined the impact of xenon on basal synaptic transmission at CA3-CA1 synapses. After 20 min of stable baseline recordings, application of 1.9 mM xenon resulted in a reduction of fEPSPs, which reached a stable plateau after approximately 15 min. Averaged slopes of fEPSPs recorded during 16–20 min after start of xenon application were 70.4 ± 3.5% compared with the normalized fEPSP slopes recorded during the last 5 min before start of xenon application (n = 7; $P = 0.001$; fig. 2A). The xenon-induced decrease of fEPSP slopes was completely reversed after removal of xenon (fig. 2A).

In a next step, we determined the action of xenon on LTP. Under control conditions, HFS potentiated fEPSP slopes to 127.2 ± 5.8% (n = 25; $P < 0.001$; fig. 3). In the presence of xenon, HFS applied *via* the second stimulation electrode produced only a short-term potentiation, and fEPSPs returned almost to baseline levels (105.9 ± 2.9%; n = 25; $P = 0.090$; fig. 3).

The effect of xenon on NMDA-EPSCs and α-amino-3-hydroxy-5-methyl-4-isoxazolepropionic acid-EPSCs was evaluated using patch-clamp recordings from CA1 stratum radiatum neurons. Xenon (1.9 mM) reduced NMDA-EPSCs to 65.9 ± 9.4% (n = 7; $P = 0.015$; fig. 4) and α-amino-3-hydroxy-5-methyl-4-isoxazolepropionic acid-EPSCs to 75.2 ± 7.6% (n = 6; $P = 0.013$; fig. 2B) of control responses. Upon termination of xenon application, the current responses recovered to the control level.

Because activation of extrasynaptic NMDA receptors is involved in the formation of LTP,[16] the influence of xenon on such receptors was investigated. The application of the glutamate reuptake inhibitor DL-threo-β-Benzyloxyaspartic acid (DL-TBOA; 30 μM) induces a pronounced spillover of glutamate, thereby also activating extrasynaptic NMDA receptors,[17] which preferentially comprise NR2B subunits.[18] To test whether the DL-TBOA–induced spillover of glutamate resulted in activation of extrasynaptic NMDA receptors, we investigated the influence of the NR2B-specific antagonist Ro-25-6981 (1 μM) on NMDA-EPSCs in the absence and presence of DL-TBOA. In the absence of DL-TBOA, Ro-25-6981 decreased the NMDA-EPSC amplitudes to 53.3 ± 4.9% of control (n = 5; $P < 0.001$; fig. 4A), whereas in the presence of DL-TBOA, Ro-25-6981 attenu-

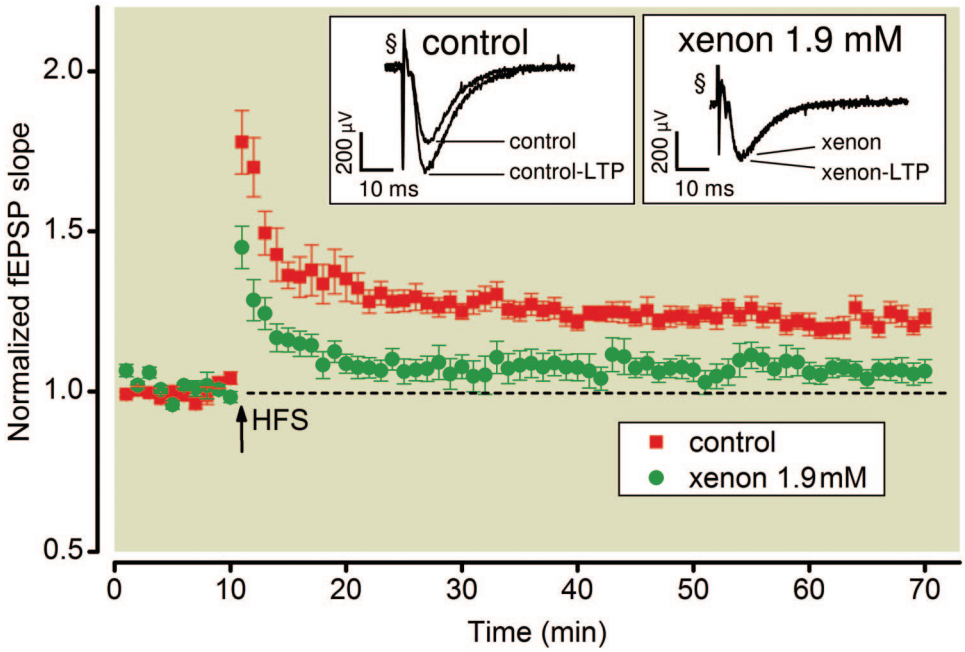

Fig. 3. Xenon blocks formation of long-term potentiation (LTP) in the hippocampus. After 10 min of stable baseline recordings, high-frequency stimulation (HFS) was applied to the Schaffer collateral-associational commissural pathway, leading to increased field excitatory postsynaptic potential (fEPSP) slopes for at least 60 min. LTP was quantified by averaging the normalized fEPSP slopes during minutes 51–60 after HFS. Under control conditions, HFS led to LTP of 127.2 ± 5.8% (95% CI 121.8–132.6; n = 25; $P < 0.001$). During application of 1.9 mM xenon, fEPSP slopes returned to baseline level after 15–20 min, showing no LTP after 60 min (105.9 ± 2.9%; 95% CI 99.09–111.9; n = 25; $P = 0.090$ *vs.* fEPSP slopes during baseline period). Each *symbol* represents the averaged fEPSP slopes normalized with respect to the 10-min baseline period before HFS. Representative recording traces (*insets*). § Stimulation artifact.

ated NMDA-EPSCs to a significantly higher degree (32.9 ± 5.7%; n = 5; $P < 0.001$; fig. 4A), pointing to an additional recruitment of extrasynaptic, NR2B-containing receptors. The xenon-induced decrease of NMDA-EPSCs was not significantly different in the presence (58.2 ± 5.8%; n = 5; $P = 0.004$; fig. 4B) or in the absence (65.9 ± 9.4%; n = 7; $P = 0.022$; fig. 4B) of DL-TBOA. These findings suggest that xenon antagonizes both synaptic and extrasynaptic NMDA receptors with the same potency.

Long-term potentiation requires an increase in intracellular calcium.[19–21] Using fluorometric calcium imaging, we tested the influence of xenon on calcium influx during HFS. Xenon reduced area-under-the-curve values to 30.2 ± 6.9% (n = 8; $P < 0.001$; fig. 5) of control. We also evaluated the effect of the specific NMDA receptor antagonist AP5 on calcium transients during HFS. AP5 nearly completely abolished fluorometric calcium signals (area under the curve 7.4 ± 2.6% of control; n = 8; $P < 0.001$; fig. 5), proving an essential role of NMDA receptors in the increase in intracellular calcium concentrations during HFS in our brain slice preparation.

In addition to NMDA receptors, an increase in intracellular calcium during HFS can be mediated *via* VGCCs, especially L-type calcium channels. Thus, we investigated the effect of xenon on calcium channel currents evoked by a depolarizing step from −70 to 0 mV in CA1 pyramidal neurons. For these experiments, the fraction of L-type calcium channels mediating the barium currents was increased pharmacologically by specific antagonists against N-, P/Q-, and T-type channels. Xenon did not affect currents recorded under these conditions (95.4 ± 7.4% of control; n = 6; $P = 0.650$; fig. 6). Coapplication of the L-type calcium channel antagonist nifedipine (5 µM) reduced calcium channel currents to 47.0 ± 13.1% and revealed a fraction of approximately 50% L-type calcium channels contributing to the entire barium current. Application of the unspecific calcium channel antagonist CdCl (100 µM) completely abolished the currents (data not shown).

Discussion

In the current study, we found that the inhalational anesthetic xenon blocks LTP in the murine hippocampus most likely by antagonizing calcium influx through NMDA receptors during HFS. Xenon antagonized synaptically and extrasynaptically located NMDA receptors with similar potency and had no effect on L-type calcium channels.

All these effects occurred under a clinically relevant concentration of xenon. Published human minimum alveolar concentrations of xenon for immobilization ($MAC_{immobility}$) are 63 vol%[22] or 71 vol%[23] and for hypnosis (MAC_{awake}) 33 vol%.[24] Using a solubility coefficient of 0.0887 at 37°C,[25] the calculated minimum alveolar concentration equivalents of dissolved xenon are 2.2 or 2.5 mM for $MAC_{immobility}$, and

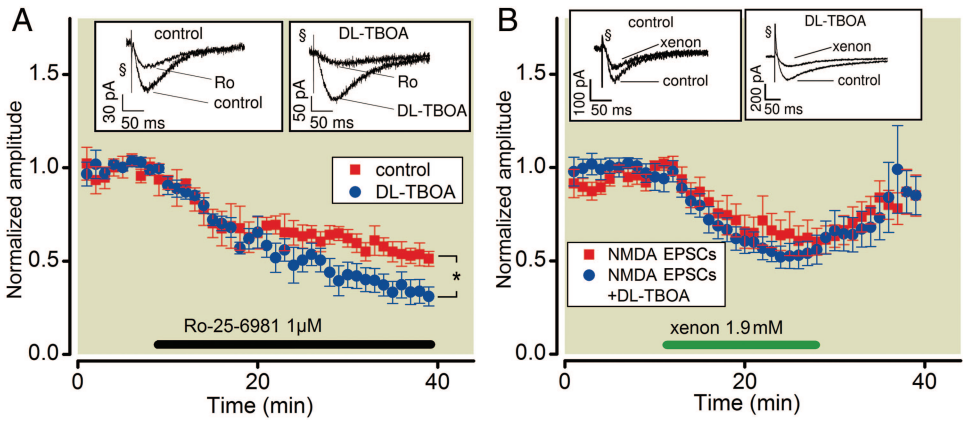

Fig. 4. Xenon attenuates *N*-methyl-D-aspartate (NMDA) receptor-mediated synaptic transmission. NMDA receptor-mediated excitatory postsynaptic currents (NMDA-EPSCs) were recorded with (*blue symbols*) and without (*red symbols*) 30 μM DL-TBOA, an antagonist of excitatory amino acid transporters. Because extrasynaptic NMDA receptors preferably contain the NR2B subunit, we applied the specific NR2B antagonist Ro-25-6981 (1 μM). Under control conditions, Ro-25-6981 led to a decrease in NMDA-EPSC amplitudes to 53.3 ± 4.9% (95% CI 39.8–66.8; n = 5; $P < 0.001$). In the presence of DL-TBOA, Ro-25-6981 reduced NMDA-EPSCs to 32.9 ± 5.7% (95% CI 16.9–48.9; n = 5; $P < 0.001$). This reduction was significantly higher ($P = 0.027$ for control *vs.* DL-TBOA), indicating that receptors containing the NR2B subunit have been activated (*A*). Xenon decreased NMDA-EPSCs (*red symbols*) to 65.9 ± 9.4% (65.9 ± 9.4%; 95% CI 43.1–88.7; n = 7; $P = 0.022$) compared with control values. Extrasynaptic NMDA receptors were activated by application of DL-TBOA. Under these conditions, xenon reduced NMDA-EPSCs to 58.2 ± 5.8% of control (*blue symbols*; 95% CI 44.2–72.2; n = 5; $P = 0.004$). Each *symbol* represents the averaged NMDA-EPSC amplitudes ± SEM normalized with respect to the 5-min baseline period before application of xenon or Ro-25-6891 (*B*). Period of substance application (*black/green bar*). Representative current traces (*insets*). § Stimulation artifact.

1.2 mM for MAC_{awake}, respectively. The applied xenon concentration of 1.9 ± 0.5 mM dissolved in aCSF at room temperature most probably resembles a concentration at which amnestic properties are likely to arise in humans. $MAC_{immobility}$ for rodents has been shown to be hyperbaric (1.61 atm[26]), so because of methodological limitations, experiments in the current study were performed at concentrations below $MAC_{immobility}$. Thus, the effects observed may

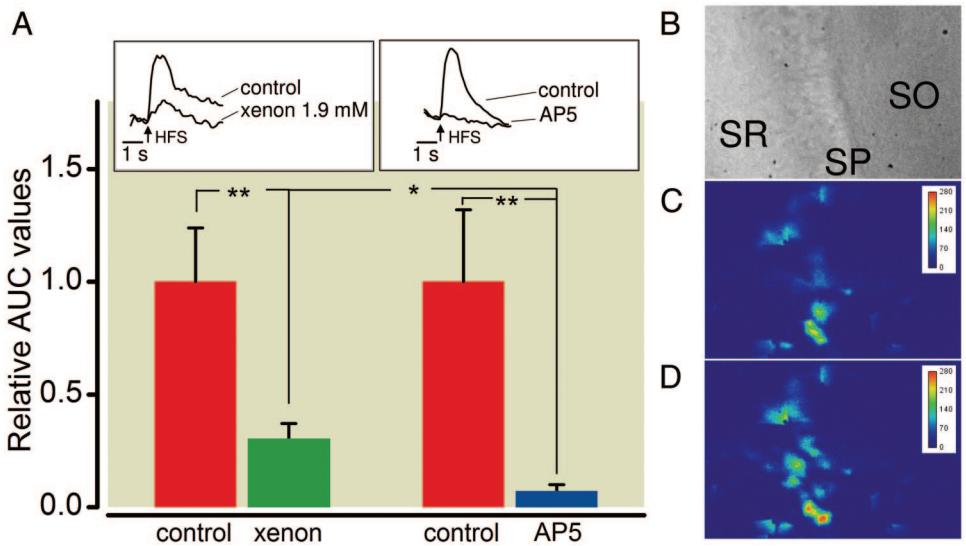

Fig. 5. Impact of xenon on intracellular calcium during high-frequency stimulation (HFS). Fluorometric calcium imaging was used to determine the increase in intracellular calcium during HFS. After 1 s of baseline recording, HFS was applied to the Schaffer collaterals, and relative changes in fluorescence were recorded for 5 s. To assess total changes in intracellular calcium, the area under the curve (AUC) was calculated. Xenon reduced the increase in intracellular calcium (30.2 ± 6.9%; 95% CI 13.9–46.5; n = 8; $P < 0.001$). Addition of the *N*-methyl-D-aspartate (NMDA) receptor antagonist AP5 to the superfusion medium completely abolished calcium transients (7.4 ± 2.6%; 95% CI 0.4–14.4; n = 8; $P < 0.001$), proving a pivotal role of NMDA receptors for intracellular calcium increase during HFS (*A*). Videomicroscopic photograph of the CA1 region of the hippocampus (*B*). Fluorescence recorded before (*C*) and during (*D*) HFS. For noise reduction, background fluorescence was subtracted. SO = stratum oriens; SP = stratum pyramidale; SR = stratum radiatum.

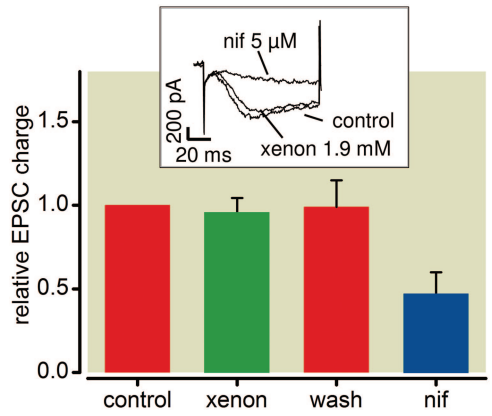

Fig. 6. Xenon does not affect L-type calcium channel currents. Depolarizing voltage steps from −70 to 0 mV evoked barium currents through calcium channels. P/Q-, N-, and T-type calcium channels were blocked pharmacologically. After stable control recordings, xenon was applied and did not change (95.4 ± 7.4% of control; 95% CI 77.7–113.1; n = 6; $P = 0.650$) the charge transfer (time integral of the current trace) through the channels. Application of the specific L-type calcium channel antagonist nifedipine (5 μM; nif) in some experiments markedly reduced the charge transfer (47.0 ± 13.1%), indicating that the recorded currents were at least to ~50% mediated by calcium channels of the L-type.

even underestimate the effects of xenon in humans under anesthesia.

Long-term potentiation, a long-lasting change in synaptic efficacy, is considered to be the major *in vitro* correlate for memory formation and learning.[4] LTP is defined as an increase in the strength of synaptic transmission measured by an increase of fEPSP slopes for at least 1 h. In accordance with this definition, xenon inhibited the induction of LTP in the CA1 region of the hippocampus.

An inhibition of hippocampal LTP by volatile anesthetics,[6,27,28] propofol,[29] and etomidate[9] has been reported. Dependent on the mechanisms of action, isoflurane,[6] sevoflurane,[7] and etomidate[9] reduce LTP, at least partly, because of their potentiating effect on the GABAergic system. In contrast, numerous reports from different laboratories suggest that xenon exerts little or no potentiating action on GABA receptor type A receptors.[30–32] Recently, it has been shown that xenon affects neurotransmission by antagonizing NMDA and α-amino-3-hydroxy-5-methyl-4-isoxazolepropionic acid receptors.[32–34] In line with these results, we provide evidence that xenon impairs LTP because of its antagonistic properties against the NMDA receptor.

Induction of LTP is NMDA receptor dependent, and an impairment of LTP has been shown for a variety of NMDA receptor antagonists.[35,36] Antagonistic properties of xenon against the NMDA receptor have been shown in other rodent central nervous system areas and in studies using heterologously expressed human NMDA receptors.[37,38] NMDA receptors are highly permeable for calcium ions, and in addition to an activation of VGCCs, the recruitment of NMDA receptors during HFS leads to an increase in the intracellular calcium concentration. It has been shown that induction of LTP can be inhibited by intracellular injection of calcium chelators.[39–41] By fluorometric calcium imaging, we could demonstrate that xenon decreases intracellular calcium influx during HFS. Two important calcium sources are involved crucially in the induction of LTP: NMDA receptors and calcium channels of the L-type.[4,5,42–47] A previous study showed no influence of xenon on L-type VGCCs in human atrial cardiomyocytes.[48] In the current study, we show that xenon did not reduce Ba^{2+}-carried currents through VGCCs when P/Q-, N-, and T-type calcium channels were antagonized pharmacologically. Nifedipine antagonized these currents to approximately 50%. (The nifedipine-resistant current probably was mediated by R-type VGCCs.[44] Unfortunately, no specific antagonists are available for this type of calcium channel current.) These results indicate that a significant fraction of this current is mediated by L-type VGCCs. Thus, an effect of xenon on L-type VGCCs in CA1 pyramidal neurons is highly unlikely.

These results suggest that the xenon-induced inhibition of LTP induction is mediated primarily by an antagonism against NMDA receptors and the resulting decrease in calcium influx during HFS. Confirmative results were obtained when NMDA receptors were blocked specifically with AP5.

Subunit composition and subunit localization of NMDA receptors changes during neuronal development. In early stages, NR2B subunits are predominantly expressed, and NR2A/NR2B ratio increases during development.[45] NR2A incorporation into the synapses replaces NR2B receptors so that in mature neurons,[46] NR2B-containing NMDA receptors are predominantly,[47] but not exclusively,[48] found in extrasynaptic receptors. At least in cortical synapses, the peak of developmental NMDA receptor remodeling can be found between postnatal days 4 and 9, and subunit expression reaches a stable state until P15.[49] Therefore, in hippocampal slices from mice used in our study (P20–30), developmental changes of subunit expression are most likely accomplished.

Synaptic NMDA receptors respond to synaptically released glutamate from the presynaptic membrane. In contrast, extrasynaptic NMDA receptors are by definition located outside synapses and are not activated by synaptic release of glutamate. They are expressed in a low surface density but represent approximately one half of the total NMDA receptor surface population.[50] Ambient glutamate has been shown to be present in a nanomolar range[51] and leads to a small tonic current mediated by extrasynaptic NMDA receptors. Extrasynaptic NMDA receptors play an important role in modulation of protein synthesis and slow network oscillations.[18] In addition, they are capable of initiating neuronal degeneration because strong activation of extrasynaptic NMDA receptors *in vivo* can contribute to calcium loading and depolarization of mitochondria that is likely to precede necrotic cell death.[52] Synaptic release of glutamate does not increase ambient glutamate concentrations, but HFS has been shown to overwhelm glutamate

reuptake transporters,[53] leading to a glutamate spillover[54] and thus increasing ambient glutamate concentrations. The maximal activation of such receptors is found at stimulation frequencies between 100 and 200 Hz[55] and resembles the HFS used in our experiments. In addition to their neurotoxic action, extrasynaptic NR2B-containing receptors are critical for the induction of synaptic plasticity because a low NR2A/NR2B ratio lowers the threshold for LTP induction, making it more likely that a modest response can increase calcium and induce LTP.[45] A reduction of extrasynaptic NMDA receptor activity has been shown to reduce neuronal degeneration[56,57] and synaptic plasticity.[58,59] It is still under debate whether synaptic NR2A-containing receptors or extrasynaptic NR2B-containing receptors are more important for the induction of LTP. A xenon-mediated reduction of extrasynaptic NMDA receptors might be an important mechanism of how xenon affects LTP in the hippocampus and how it mediates its neuroprotective properties.

Spillover of glutamate predominantly activates NR2B-containing NMDA receptors.[16,60,61] In fact, when glutamate transporters were blocked, the NR2B subunit-selective antagonist Ro-25-6981 reduced NMDA-EPSCs more extensively, demonstrating that extrasynaptic NR2B-containing NMDA receptors also had been activated. The allosteric NMDA receptor antagonist Ro-25-6981 has a 3,000-fold selectivity of NR1/NR2B NMDA receptors over NR1/NR2A receptors.[62] An activity against NR2A-containing receptors has been reported for high concentrations with an IC_{50} greater than 30 μM.[62] In contrast, IC_{50} for NR2B-containing NMDA receptors is reported to be 0.009 μM. The concentration used in our experiments (1 μM) is far below the IC_{50} for NR2A-containing NMDA receptors but in the range of selective concentrations (0.5–3 μM)[63] for NR2B-containing NMDA receptors. It has been shown recently that synaptically located NMDA receptors were antagonized by xenon nonselectively for receptors containing either the NR2A or NR2B subunit.[12] Although we were not able to record currents from isolated extrasynaptic NMDA receptors, we could demonstrate that DL-TBOA increased the fraction of NR2B-containing extrasynaptic NMDA receptors governing NMDA-EPSCs. Under these experimental conditions, the application of xenon antagonized NMDA-EPSCs with similar potency as in the absence of DL-TBOA. This shows that xenon exerts no specificity to synaptically or extrasynaptically located NMDA receptors. These results are in line with previous studies showing that xenon affects NMDA receptors regardless of subunit composition (NR2A or NR2B)[12] and inhibits NMDA receptors, presumably by binding to the glycine site at the NR1 subunit.[64]

Extrasynaptic GABA receptor type A receptors are also expressed in the hippocampus and are critically involved in learning and memory processes.[65] However, there is increasing evidence that xenon does not affect GABA receptor type A receptors, so that possible amnestic actions of xenon are highly unlikely to be mediated by a modulation of extrasynaptic GABA receptor type A receptors.

It has been suggested that attenuation of synaptic plasticity in the hippocampus may contribute to the amnestic properties of anesthetics.[6,7,9] Although LTP in the hippocampus is accepted to underlie certain forms of memory (*e.g.*, spatial learning[42]), other mechanisms and brain regions also contribute to memory formation and recall.[66,67] However, recent work[3] could demonstrate a participation of the hippocampus in the amnestic action produced by propofol. Impairment of memory formation during surgery is one of the key properties of anesthesia. Meanwhile, xenon anesthesia in humans has been evaluated in a number of clinical trials[10,11,68] and studies using healthy volunteers.[69,70] In none of these studies has the occurrence of awareness during xenon anesthesia been systematically investigated, and to our knowledge no case of intraoperative awareness has been reported. Given the lack of a systemic investigation and the small numbers of patients included in these trials, it is too early to draw a definite conclusion as to whether xenon has less or more amnestic potency than do other inhalative anesthetics. However, apparently a prevention of intraoperative memory formation occurs during xenon anesthesia. The demonstrated xenon-induced attenuation of hippocampal LTP most probably is attributable to an antagonism against NMDA receptors and represents one mechanism of how the inhalative anesthetic xenon exerts its amnestic properties and prevents patients from undesirable intraoperative memory formation.

The authors thank Alexander Yassouridis, Ph.D. (Biostatistician, Head of the Research Group Biostatistics, Max Planck Institute of Psychiatry, Munich, Germany), for statistical advice.

References

1. Errando CL, Sigl JC, Robles M, Calabuig E, García J, Arocas F, Higueras R, Del Rosario E, López D, Peiró CM, Soriano JL, Chaves S, Gil F, García-Aguado R: Awareness with recall during general anaesthesia: A prospective observational evaluation of 4001 patients. Br J Anaesth 2008; 101:178–85
2. Alkire MT, Nathan SV: Does the amygdala mediate anesthetic-induced amnesia? Basolateral amygdala lesions block sevoflurane-induced amnesia. Anesthesiology 2005; 102:754–60
3. Ren Y, Zhang FJ, Xue QS, Zhao X, Yu BW: Bilateral inhibition of gamma-aminobutyric acid type A receptor function within the basolateral amygdala blocked propofol-induced amnesia and activity-regulated cytoskeletal protein expression inhibition in the hippocampus. Anesthesiology 2008; 109:775–81
4. Bliss TV, Collingridge GL: A synaptic model of memory: Long-term potentiation in the hippocampus. Nature 1993; 361:31–9
5. Grover LM, Teyler TJ: Differential effects of NMDA receptor antagonist APV on tetanic stimulation induced and calcium induced potentiation. Neurosci Lett 1990; 113:309–14
6. Simon W, Hapfelmeier G, Kochs E, Zieglgänsberger W, Rammes G: Isoflurane blocks synaptic plasticity in the mouse hippocampus. Anesthesiology 2001; 94:1058–65
7. Ishizeki J, Nishikawa K, Kubo K, Saito S, Goto F: Amnestic concentrations of sevoflurane inhibit synaptic plasticity of hippocampal CA1 neurons through gamma-aminobutyric acid-mediated mechanisms. Anesthesiology 2008; 108:447–56

8. Nagashima K, Zorumski CF, Izumi Y: Propofol inhibits long-term potentiation but not long-term depression in rat hippocampal slices. ANESTHESIOLOGY 2005; 103:318–26
9. Martin LJ, Oh GH, Orser BA: Etomidate targets alpha5 gamma-aminobutyric acid subtype A receptors to regulate synaptic plasticity and memory blockade. ANESTHESIOLOGY 2009; 111:1025–35
10. Rossaint R, Reyle-Hahn M, Schulte Am Esch J, Scholz J, Scherpereel P, Vallet B, Giunta F, Del Turco M, Erdmann W, Tenbrinck R, Hammerle AF, Nagele P, Xenon Study Group: Multicenter randomized comparison of the efficacy and safety of xenon and isoflurane in patients undergoing elective surgery. ANESTHESIOLOGY 2003; 98:6–13
11. Wappler F, Rossaint R, Baumert J, Scholz J, Tonner PH, van Aken H, Berendes E, Klein J, Gommers D, Hammerle A, Franke A, Hofmann T, Schulte Esch J, Xenon Multicenter Study Research Group: Multicenter randomized comparison of xenon and isoflurane on left ventricular function in patients undergoing elective surgery. ANESTHESIOLOGY 2007; 106:463–71
12. Haseneder R, Kratzer S, Kochs E, Höfelmann D, Auberson Y, Eder M, Rammes G: The xenon-mediated antagonism against the NMDA receptor is non-selective for receptors containing either NR2A or NR2B subunits in the mouse amygdala. Eur J Pharmacol 2009; 619:33–7
13. Anderson WW, Collingridge GL: The LTP Program: A data acquisition program for on-line analysis of long-term potentiation and other synaptic events. J Neurosci Methods 2001; 108:71–83
14. Dodt HU, Eder M, Schierloh A, Zieglgänsberger W: Infrared-guided laser stimulation of neurons in brain slices. Sci STKE 2002; 2002:pl2
15. Gee KR, Brown KA, Chen WN, Bishop-Stewart J, Gray D, Johnson I: Chemical and physiological characterization of fluo-4 Ca(2+)-indicator dyes. Cell Calcium 2000; 27:97–106
16. Lozovaya NA, Grebenyuk SE, Tsintsadze TSh, Feng B, Monaghan DT, Krishtal OA: Extrasynaptic NR2B and NR2D subunits of NMDA receptors shape 'superslow' afterburst EPSC in rat hippocampus. J Physiol 2004; 558:451–63
17. Tzingounis AV, Wadiche JI: Glutamate transporters: Confining runaway excitation by shaping synaptic transmission. Nature Reviews Neuroscience 2007; 8:935–47
18. Groc L, Bard L, Choquet D: Surface Trafficking of *N*-methyl-D-aspartate receptors: Physiological and pathological perspectives. Neuroscience 2009; 158:4–18
19. Harney SC, Rowan M, Anwyl R: Long-term depression of NMDA receptor-mediated synaptic transmission is dependent on activation of metabotropic glutamate receptors and is altered to long-term potentiation by low intracellular calcium buffering. J Neurosci 2006; 26:1128–32
20. Kwon HB, Castillo PE: Long-term potentiation selectively expressed by NMDA receptors at hippocampal mossy fiber synapses. Neuron 2008; 57:108–20
21. Rebola N, Lujan R, Cunha RA, Mulle C: Adenosine A2A receptors are essential for long-term potentiation of NMDA-EPSCs at hippocampal mossy fiber synapses. Neuron 2008; 57:121–34
22. Cullen SC, Eger EI 2nd, Cullen BF, Gregory P: Observations on the anesthetic effect of the combination of xenon and halothane. ANESTHESIOLOGY 1969; 31:305–9
23. Nakata Y, Goto T, Ishiguro Y, Terui K, Kawakami H, Santo M, Niimi Y, Morita S: Minimum alveolar concentration (MAC) of xenon with sevoflurane in humans. ANESTHESIOLOGY 2001; 94:611–4
24. Goto T, Nakata Y, Saito H, Ishiguro Y, Niimi Y, Suwa K, Morita S: Bispectral analysis of the electroencephalogram does not predict responsiveness to verbal command in patients emerging from xenon anaesthesia. Br J Anaesth 2000; 85:359–63
25. Weathersby PK, Homer LD: Solubility of inert gases in biological fluids and tissues: A review. Undersea Biomed Res 1980; 7:277–96
26. Koblin DD, Fang Z, Eger EI 2nd, Laster MJ, Gong D, Ionescu P, Halsey MJ, Trudell JR: Minimum alveolar concentrations of noble gases, nitrogen, and sulfur hexafluoride in rats: Helium and neon as nonimmobilizers (nonanesthetics). Anesth Analg 1998; 87:419–24
27. Haseneder R, Kratzer S, von Meyer L, Eder M, Kochs E, Rammes G: Isoflurane and sevoflurane dose-dependently impair hippocampal long-term potentiation. Eur J Pharmacol 2009; 623:47–51
28. Otsubo T, Maekawa M, Nagai T, Sakio H, Hori Y: Facilitatory effects of subanesthetic sevoflurane on excitatory synaptic transmission and synaptic plasticity in the mouse hippocampal CA1 area. Brain Res 2008; 1197:32–9
29. Takamatsu I, Sekiguchi M, Wada K, Sato T, Ozaki M: Propofol-mediated impairment of CA1 long-term potentiation in mouse hippocampal slices. Neurosci Lett 2005; 389:129–32
30. de Sousa SL, Dickinson R, Lieb WR, Franks NP: Contrasting synaptic actions of the inhalational general anesthetics isoflurane and xenon. ANESTHESIOLOGY 2000; 92:1055–66
31. Franks NP, Dickinson R, de Sousa SL, Hall AC, Lieb WR: How does xenon produce anaesthesia? Nature 1998; 396:324
32. Haseneder R, Kratzer S, Kochs E, Eckle VS, Zieglgänsberger W, Rammes G: Xenon reduces *N*-methyl-D-aspartate and alpha-amino-3-hydroxy-5-methyl-4-isoxazolepropionic acid receptor-mediated synaptic transmission in the amygdala. ANESTHESIOLOGY 2008; 109:998–1006
33. Haseneder R, Kratzer S, Kochs E, Mattusch C, Eder M, Rammes G: Xenon attenuates excitatory synaptic transmission in the rodent prefrontal cortex and spinal cord dorsal horn. ANESTHESIOLOGY 2009; 111:1297–307
34. Nagele P, Metz LB, Crowder CM: Xenon acts by inhibition of non-*N*-methyl-D-aspartate receptor-mediated glutamatergic neurotransmission in *Caenorhabditis elegans*. ANESTHESIOLOGY 2005; 103:508–13
35. Coan EJ, Saywood W, Collingridge GL: MK-801 blocks NMDA receptor-mediated synaptic transmission and long term potentiation in rat hippocampal slices. Neurosci Lett 1987; 80:111–4
36. Bashir ZI, Tam B, Collingridge GL: Activation of the glycine site in the NMDA receptor is necessary for the induction of LTP. Neurosci Lett 1990; 108:261–6
37. Ogata J, Shiraishi M, Namba T, Smothers CT, Woodward JJ, Harris RA: Effects of anesthetics on mutant *N*-methyl-D-aspartate receptors expressed in *Xenopus* oocytes. J Pharmacol Exp Ther 2006; 318:434–43
38. Yamakura T, Harris RA: Effects of gaseous anesthetics nitrous oxide and xenon on ligand-gated ion channels. Comparison with isoflurane and ethanol. ANESTHESIOLOGY 2000; 93:1095–101
39. Hüneke R, Jüngling E, Skasa M, Rossaint R, Lückhoff A: Effects of the anesthetic gases xenon, halothane, and isoflurane on calcium and potassium currents in human atrial cardiomyocytes. ANESTHESIOLOGY 2001; 95:999–1006
40. Lynch G, Larson J, Kelso S, Barrionuevo G, Schottler F: Intracellular injections of EGTA block induction of hippocampal long-term potentiation. Nature 1983; 305:719–21
41. Bröcher S, Artola A, Singer W: Intracellular injection of Ca2+ chelators blocks induction of long-term depression in rat visual cortex. Proc Natl Acad Sci USA 1992; 89:123–7
42. Morris RG, Anderson E, Lynch GS, Baudry M: Selective impairment of learning and blockade of long-term potentiation by an *N*-methyl-D-aspartate receptor antagonist, AP5. Nature 1986; 319:774–6
43. Morgan SL, Teyler TJ: VDCCs and NMDARs underlie two forms of LTP in CA1 hippocampus *in vivo*. Journal of Neurophysiology 1999; 82:736–40

44. Sochivko D, Chen J, Becker A, Beck H: Blocker-resistant Ca2+ currents in rat CA1 hippocampal pyramidal neurons. Neuroscience 2003; 116:629–38
45. Yashiro K, Philpot BD: Regulation of NMDA receptor subunit expression and its implications for LTD, LTP, and metaplasticity. Neuropharmacology 2008; 55:1081–94
46. Gambrill AC, Barria A: NMDA receptor subunit composition controls synaptogenesis and synapse stabilization. Proc Natl Acad Sci USA 2011; 108:5855–60
47. Li B, Chen N, Luo T, Otsu Y, Murphy TH, Raymond LA: Differential regulation of synaptic and extra-synaptic NMDA receptors. Nature Neuroscience 2002; 5:833–4
48. Thomas CG, Miller AJ, Westbrook GL: Synaptic and extrasynaptic NMDA receptor NR2 subunits in cultured hippocampal neurons. J Neurophysiol 2006; 95:1727–34
49. Liu L, Wong TP, Pozza MF, Lingenhoehl K, Wang Y, Sheng M, Auberson YP, Wang YT: Role of NMDA receptor subtypes in governing the direction of hippocampal synaptic plasticity. Science 2004; 304:1021–4
50. Groc L, Heine M, Cousins SL, Stephenson FA, Lounis B, Cognet L, Choquet D: NMDA receptor surface mobility depends on NR2A–2B subunits. Proc Natl Acad Sci USA 2006; 103:18769–74
51. Herman MA, Jahr CE: Extracellular glutamate concentration in hippocampal slice. J Neurosci 2007; 27:9736–41
52. Hardingham GE, Bading H: The Yin and Yang of NMDA receptor signalling. Trends Neurosci 2003; 26:81–9
53. Diamond JS, Jahr CE: Synaptically released glutamate does not overwhelm transporters on hippocampal astrocytes during high-frequency stimulation. J Neurophysiol 2000; 83: 2835–43
54. Kullmann DM, Asztely F: Extrasynaptic glutamate spillover in the hippocampus: Evidence and implications. Trends Neurosci 1998; 21:8–14
55. Harris AZ, Pettit DL: Recruiting extrasynaptic NMDA receptors augments synaptic signaling. J Neurophysiol 2008; 99: 524–33
56. Babu CS, Ramanathan M: Pre-ischemic treatment with memantine reversed the neurochemical and behavioural parameters but not energy metabolites in middle cerebral artery occluded rats. Pharmacol Biochem Behav 2009; 92:424–32
57. Xia P, Chen HS, Zhang D, Lipton SA: Memantine preferentially blocks extrasynaptic over synaptic NMDA receptor currents in hippocampal autapses. J Neurosci 2010; 30: 11246–50
58. Clayton DA, Mesches MH, Alvarez E, Bickford PC, Browning MD: A hippocampal NR2B deficit can mimic age-related changes in long-term potentiation and spatial learning in the Fischer 344 rat. J Neurosci 2002; 22:3628–37
59. Bartlett TE, Bannister NJ, Collett VJ, Dargan SL, Massey PV, Bortolotto ZA, Fitzjohn SM, Bashir ZI, Collingridge GL, Lodge D: Differential roles of NR2A and NR2B-containing NMDA receptors in LTP and LTD in the CA1 region of two-week old rat hippocampus. Neuropharmacology 2007; 52:60–70
60. Scimemi A, Fine A, Kullmann DM, Rusakov DA: NR2B-containing receptors mediate cross talk among hippocampal synapses. J Neurosci 2004; 24:4767–77
61. Rusakov DA, Scimemi A, Walker MC, Kullmann DM: Comment on "Role of NMDA receptor subtypes in governing the direction of hippocampal synaptic plasticity." Science 2004; 305:1912
62. Neyton J, Paoletti P: Relating NMDA receptor function to receptor subunit composition: Limitations of the pharmacological approach. J Neurosci 2006; 26:1331–3
63. Mutel V, Buchy D, Klingelschmidt A, Messer J, Bleuel Z, Kemp JA, Richards JG: In vitro binding properties in rat brain of [3H]Ro 25–6981, a potent and selective antagonist of NMDA receptors containing NR2B subunits. J Neurochem 1998; 70:2147–55
64. Dickinson R, Peterson BK, Banks P, Simillis C, Martin JC, Valenzuela CA, Maze M, Franks NP: Competitive inhibition at the glycine site of the *N*-methyl-D-aspartate receptor by the anesthetics xenon and isoflurane: Evidence from molecular modeling and electrophysiology. ANESTHESIOLOGY 2007; 107: 756–67
65. Martin LJ, Zurek AA, MacDonald JF, Roder JC, Jackson MF, Orser BA: Alpha5GABAA receptor activity sets the threshold for long-term potentiation and constrains hippocampus-dependent memory. J Neurosci 2010; 30:5269–82
66. Hölscher C: Synaptic plasticity and learning and memory: LTP and beyond. J Neurosci Res 1999; 58:62–75
67. Martin SJ, Grimwood PD, Morris RG: Synaptic plasticity and memory: An evaluation of the hypothesis. Annu Rev Neurosci 2000; 23:649–711
68. Lachmann B, Armbruster S, Schairer W, Landstra M, Trouwborst A, Van Daal GJ, Kusuma A, Erdmann W: Safety and efficacy of xenon in routine use as an inhalational anaesthetic. Lancet 1990; 335:1413–5
69. Laitio RM, Kaskinoro K, Särkelä MO, Kaisti KK, Salmi E, Maksimow A, Långsjö JW, Aantaa R, Kangas K, Jääskeläinen S, Scheinin H: Bispectral index, entropy, and quantitative electroencephalogram during single-agent xenon anesthesia. ANESTHESIOLOGY 2008; 108:63–70
70. Bedi A, McCarroll C, Murray JM, Stevenson MA, Fee JP: The effects of subanaesthetic concentrations of xenon in volunteers. Anaesthesia 2002; 57:233–41